Electronic Journal of Statistics
Vol. 11 (2017) 1949–1982
ISSN: 1935-7524
DOI: 10.1214/17-EJS1235

Statistical models for cores decomposition of an undirected random graph

Vishesh Karwa*

Carnegie Mellon University and Harvard University
e-mail: vkarwa@seas.harvard.edu

Michael J. Pelsmajer*, **Sonja Petrović***, **Despina Stasi*** **and Dane Wilburne***

Illinois Institute of Technology
e-mail: pelsmajer@iit.edu; sonja.petrovic@iit.edu
stasdes@iit.edu; dwilburn@hawk.iit.edu

Abstract: The k-core decomposition is a widely studied summary statistic that describes a graph's global connectivity structure. In this paper, we move beyond using k-core decomposition as a tool to summarize a graph and propose using k-core decomposition as a tool to model random graphs. We propose using the shell distribution vector, a way of summarizing the decomposition, as a sufficient statistic for a family of exponential random graph models. We study the properties and behavior of the model family, implement a Markov chain Monte Carlo algorithm for simulating graphs from the model, implement a direct sampler from the set of graphs with a given shell distribution, and explore the sampling distributions of some of the commonly used complementary statistics as good candidates for heuristic model fitting. These algorithms provide first fundamental steps necessary for solving the following problems: parameter estimation in this ERGM, extending the model to its Bayesian relative, and developing a rigorous methodology for testing goodness of fit of the model and model selection. The methods are applied to a synthetic network as well as the well-known Sampson monks dataset.

Received October 2015.

1. Introduction

Network analyses are often concerned—either directly or indirectly—with the degrees of the nodes in the network, a natural approach since counting the number of edges incident to a node gives a basic local measure of connectivity. Several familiar statistical frameworks assign a probability distribution to the set of networks on a fixed number of nodes based on their degree information, e.g. Holland and Leinhardt (1981), Chatterjee et al. (2011), Olhede and Wolfe (2012), and Rinaldo et al. (2013). However, despite the rich structure degree-based models offer compared to simpler models such as Erdös-Renyi-Gilbert,

*Authors are listed in alphabetical order; contributions are equal.

they fail to capture certain vital connectivity information about the network. In some applications, it matters not just to how many other nodes a particular node in the network is connected, but also to *which* other nodes it is connected. For example, a node v may seem important if it has high degree, but if all its neighbors are themselves unimportant due to having no additional connections (e.g., if they all have degree 1), then the "influence" or "centrality" of v within the network is not actually all that impressive, after all. This distinction is especially crucial in applications concerning information dispersal as in Pei et al. (2012), the spread of infectious diseases or viruses as in Kitsak et al. (2010), or robustness to node failure. In the social network context, this importance can be interpreted as "celebrity status" of a node. Whereas degree-centric analyses are not well-suited to model such situations, the *core decomposition* of a network graph can capture precisely this type of information.

Cores of a graph were introduced by Seidman (1983) to study tightly-knit groups in social networks. Since then, core decomposition has been used as a tool for numerous applications varying from understanding protein networks (Wuchty and Almaas, 2005), visualization of large networks (Alvarez-Hamelin et al., 2006), and understanding the topology of the Internet graph (Carmi et al., 2007) to name a few. In studies such as Kitsak et al. (2010) and Bae and Kim (2014), the authors identify spreader nodes and rank them in terms of their spreading influence, using a graph's core decomposition. Methods for identifying spreaders using cores were extended to dynamic networks in Miorandi and Pellegrini (2010) and core decomposition in general was extended to weighted networks in Eidsaa and Almaas (2013). An important feature of a core decomposition is that it can be computed efficiently (see, e.g., Lee et al. (2013)), even for "uncertain graphs" which are graphs whose edges have some probability of existing–such graphs have applications in biological networks that model, for instance, protein interactions (see Bonchi et al. (2014)). Although core decomposition has become an important and widely used tool as a descriptive summary statistic of the network, it is a statistic for which there does not exist an associated statistical model.

The goal of this paper is to place the core decomposition of a network on a rigorous statistical foundation and present it as a tool for statistical modeling rather than descriptive analysis. We construct a natural model based on core decomposition by embedding the core structure of a graph in the family of exponential random graph models (ERGMs) and describe its theoretical properties. We restrict the support of the model to allow only networks with a fixed *degeneracy* to have a positive probability. We show that this eliminates certain bad properties common to many ERGMs and expect that such support restrictions may help improve the properties of other ERGMs as well. We study three common inference tasks as they apply to the support-restricted ERGM: sampling, maximum likelihood estimation, and goodness-of-fit testing. More specifically, the contributions of this paper are as follows:

1. In Section 2, we summarize the core decomposition of a network in the form of a *shell distribution*, and in Section 3 we introduce a *support-*

restricted exponential random graph model with the shell distribution as a sufficient statistic.
2. In Section 4, we perform simulation studies to understand the behavior of the model by relying on an MCMC algorithm to sample from the model and to estimate the parameters of the model.
3. In Section 5, we present an algorithm to sample from the space of graphs given a fixed shell distribution.
4. We return to the theoretical properties of the model in Sections 6 and 7, where we study the space of graphs with a fixed shell distribution and describe the *marginal polytope* associated with the model and conditions for the existence of MLE, respectively.

ERGMs provide a natural framework to model networks through their sufficient statistics; see Robins et al. (2007) for an introduction. Goldenberg et al. (2009) provide a comprehensive review of various ways to model networks, including ERGMs. ERGMs are a special case of the venerable class of exponential families which are known to possess excellent statistical properties; see Brown (1986) for a theoretical treatment of exponential families and Rinaldo et al. (2009) in particular for discrete exponential family models, including ERGMs. ERGMs have been the workhorse of many applied studies and the literature is too vast to be surveyed here; see Snijders et al. (2006); Saul and Filkov (2007) and Goodreau et al. (2009) for examples of studies that use ERGMs for network modeling.

Our goal is to add to the toolbox of ERGMs the ability to model the core structure of a graph. Doing so has two important consequences: First, it puts the core structure of a graph, summarized by its shell distribution, on a firm statistical footing. Second, it allows us to understand what properties of a network are captured by the shell distribution. It is worth noting that any ERGM based on a core decomposition *cannot* be specialized to the Erdös-Rényi model, i.e., the Erdös-Rényi model is not a submodel of any ERGM based on the core decomposition. In fact, the same is true for any ERGM with sufficient statistics based on the degree sequence of the network. As such, the shell distribution ERGM would occupy a unique space in the network literature. Models based on the core distribution go beyond the dyadic independence assumption inherent in the degree-sequence-based network models and are able to capture transitivity effects. These models differ from the ERGM-based subgraph counts, such as triangles and stars, which also go beyond the dyadic independence assumption. This is because the core structure of a network is a *global* sufficient statistic in the following sense: to which core a node belongs depends in some way on the entire network; see Section 2 for the precise definition of a core and some examples. In contrast, subgraph counts measure local and coarse properties of the network.

We want to point out that for all the good properties of ERGMs, they are not without drawbacks. Recent empirical and theoretical work has brought to light some undesirable properties of some special classes of ERGMs; these properties are often termed as "model degeneracy" (Rinaldo et al. (2009); Schwein-

berger (2011); Chatterjee and Diaconis (2013); Hunter et al. (2008)) or "inconsistency" (Shalizi et al. (2013)). As noted in Rinaldo et al. (2009), "model degeneracy" is an umbrella term used to denote many undesirable properties of ERGMs. One specific drawback to note is that it may be difficult to sample efficiently (Bannister et al.), but that is an issue for ERGMs in general and outside the scope of this paper. We discuss these issues in Section 9.2 and explain how we fix them by placing support restrictions on the class of models that we consider. Since the word degeneracy also refers to a graph-theoretic notion which is relevant to this work, we avoid the use of the term "model degeneracy" and instead use the term "bad behavior" of the model.

2. Technical preliminaries: Cores and shells

We restrict our analysis to the set of *simple* graphs, representing networks without multiple edges and self-loops. For the remainder of this manuscript, let $\mathcal{G}_n$ denote the set of all simple graphs on n nodes. We are interested in distributions over the set $\mathcal{G}_n$; thus G will denote a random variable with state space $\mathcal{G}_n$, and $G = g$ its realization. We will also consider families of subsets of $\mathcal{G}_n$ below.

Definition 1 (Seidman (1983))**.** The *k-core* of a graph g, denoted by $H_k(g)$ or simply H_k if the graph is clear from the context, is the maximal subgraph in which every vertex has degree at least k[1].

As it is often useful to think of the k-core as the output of an algorithm for which the graph g is the input, we also use the equivalent algorithmic definition: H_k is the subgraph obtained by iteratively deleting vertices of degree less than k; see Algorithm 1. For example, for the particular graph $G = g$ on the left of Figure 1, $H_0(g)$ is just the graph itself, H_1 is g without the isolated vertex, the 2-core H_2 is shown in the middle, and H_3 and H_4 both are the graph shown on the right. For $k \geq 5$, H_k is the empty graph.

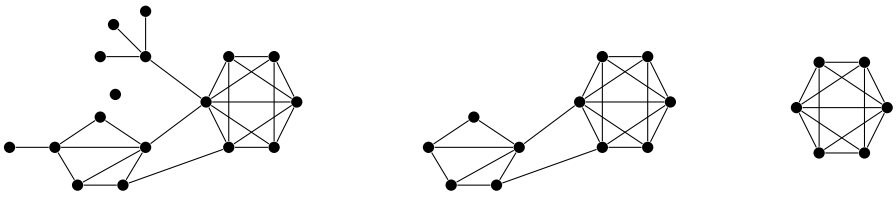

FIG 1. *A small graph g (left), its 2-core (center), and its 3- and 4-core (right).*

Each node is contained in several k-cores, for every k from 0 to whatever the largest k is for that node. Thus, the following node statistic captures all core information for a node.

[1]This is the usual definition of the k-core and it appropriately describes the notion of node importance and robust degree. Seidman's original definition also requires the subgraph to be connected.

Definition 2. A vertex v in a graph g has *shell index* i if $v \in H_i(g)$ but $v \notin H_{i+1}(g)$. Define $s_g : V \to \mathbb{N}$ as the function that maps vertices of g to the non-negative integers according to their shell indices, so that if v has shell index i we may write $s_g(v) = i$. If the graph g is clear from the context, we drop the subscript and simply write $s(v) = i$.

In other words, the shell index of a vertex v indicates the highest core to which v belongs. For example, not all nodes in the 2-core $H_2(g)$ in the middle of Figure 1 have shell index 2 in g: the six nodes on the right have shell index 4. The vertex set $V(g)$ of any network g can be partitioned according to the shell indices, since the shell index exists, is well-defined and is unique for all vertices. There are two natural ways to record all of the shell index information about a network, and hence, record the information that captures its core structure. First, the *shell sequence* $s(g)$ of an n-vertex graph g with vertices $v_1, \ldots, v_n$ is a vector of length n whose i^{th} entry is the shell index of vertex v_i. Second, if the interest is in unlabeled graphs (i.e., exchangeable models for labeled graphs), it is natural to summarize the sequence with a histogram as follows. The *shell distribution* $n_S(g)$ of an n-vertex graph g is a vector of length n whose j^{th} entry $n_j(g)$ is the number of vertices of g that have shell index j, for $0 \leq j \leq n-1$. Note that the shell index of a vertex is bounded above by its degree, which is bounded above by $n-1$. Thus $\sum_{j=0}^{n-1} n_j(g) = n$. In symbols,

$$n_S(g) := (n_0(g), n_1(g), \ldots, n_{n-1}(g)),$$

where $n_j(g) = |\{v \in V(g) : s(v) = j,\ 0 \leq j \leq n-1\}|$. For example, the graphs in Figures 2(a) and 2(b) both have shell distribution $(0, 8, 0, 0, 0, 0, 0, 0)$. The graphs in Figures 2(c) and 2(d) have shell distributions $(0, 0, 8, 0, 0, 0, 0, 0)$ and $(0, 0, 4, 4, 0, 0, 0, 0)$, respectively. These graphs illustrate the fact that the degree and core structures of a graph are not obtainable from one another. Graph g of Figure 1 has shell distribution $(1, 5, 5, 0, 6, 0, 0, 0, 0, 0, 0, 0, 0, 0)$.

(a) Vertices have degrees 1, 2, and 3.

(b) All eight vertices have degree 1.

(c) All vertices belong to the 0-core, 1-core and 2-core. Higher cores are empty.

(d) All vertices are in k-core for $k = 0, 1, 2$, but 4 of the vertices are also in the 3-core.

FIG 2. *The graphs in (a) and (b) have the same core structure but different degree structure. The graphs in (c) and (d) have the same degree structure but different core structure.*

Finally, the *degeneracy* of a graph $g \in \mathcal{G}_n$, denoted by $\text{dgen}(g)$, is the index of the largest nonzero entry in the shell distribution vector $n_S(g)$. In other words, the degeneracy of a graph is the maximum index of a non-empty shell. Thus we may define the following subset of the set of simple n-vertex graphs $\mathcal{G}_n$:

$$\mathcal{G}_{n,m} = \{g \in \mathcal{G}_n : \text{dgen}(g) = m\}.$$

3. The shell distribution ERGM

A natural way to model random graphs using their core structure is to embed summaries of their core structure in the exponential random graph model (ERGM) framework. In what follows, we define a family of ERGMs using one such summary, namely the shell distribution, as a sufficient statistic.

Let $G = g$ be an instance of a random graph from the set $\mathcal{G}_n$. Partitioning the vertex set of g according to the shell indices implies that the probability of observing g is

$$P(G = g; p) = (\varphi(p))^{-1} \prod_{j=0}^{n-1} p_j^{n_j(g)}, \tag{1}$$

where $p_j \in (0, 1)$ is the parameter that represents the propensity of shell j to have vertices in it, $p = (p_0, p_1, \ldots, p_{n-1})$ is the parameter vector, integers $n_j(g)$ are the components of the shell distribution vector $n_S(g)$ as defined above, and $\varphi(p)$ is the partition function. [One may also think of p_j as representing the *attractiveness* of shell j.] Note that a feature of the model is that there is no dyad independence assumption. Equation (1) is a most direct way to define an ERGM based on the shell distribution. One can easily see that it can be written in exponential family form (see Appendix 9), which allows us to take advantage of various good properties of exponential families.

It turns out, however, that specification (1) of the model has many undesirable properties, common to other ERGMs (Rinaldo et al., 2009); details are given in Appendix 9. There are several ways to avoid these issues that arise from specifying the model as in Equation (1); one such way is to add an additional parameter to the model as follows. We restrict the support of the model to the set $\mathcal{G}_{n,m}$ of all simple graphs whose degeneracy is equal to m.

$$P(G = g; p, m) = \begin{cases} (\varphi(p))^{-1} \prod_{j=0}^{m} p_j^{n_j(g)} & \text{if } g \in \mathcal{G}_{n,m}, \\ 0 & \text{otherwise,} \end{cases} \tag{2}$$

where

$$\varphi(p) = \sum_{g \in \mathcal{G}_{n,m}} \prod_{j=0}^{m} p_j^{n_j(g)}$$

is the normalizing constant (partition function). Equation (2) defines a multinomial-like distribution over the partition of nodes induced by the shell distribution. By limiting degeneracy, the model has a significantly reduced number of parameters, which offers an additional advantage in estimation over the more general model.

For each fixed value m of degeneracy, the model defined by Equation (2) is an ERGM supported on the subset of graphs $\mathcal{G}_{n,m}$. We have thus defined a family of models with parameters p and m, where $p = (p_0, \ldots, p_m) \in \Delta_{m+1}$ and $m \in \{0, \ldots, n-1\}$. It is a union of ERGMs, one for each distinct value of m.

For the remainder of the paper, this support restriction is assumed to be present and made implicit, unless otherwise mentioned, to ease notation. The dimension of the parameter space is $m + 1$ and is a function of the parameter m.

Remark 3. In this paper, we will treat m as fixed and known. When fitting the model to real networks, m will be selected by setting it equal to the degeneracy of the observed graph, assuming the sample size $N = 1$ as is most common in applications. Estimating m and fitting the shell ERGM when $N > 1$ and the observed graphs have distinct degeneracy values is an open question. The choice of fixing m rather than treating it as an estimable parameter is both reasonable and warranted. The degeneracy of a graph is an important metric that describes its sparsity and is easily calculable from the data. If the degeneracy is not fixed, the large majority of model parameters will not be estimable, as the observed graphs are expected to be sparse (real networks usually are), with observed degeneracy much smaller than N; see also Section 4.1. Moreover, simulations show that allowing m to be different from the observed degeneracy leads to a poorly behaved model, as explained in Section 9.2. Intuitively, having $p_i > 0$ for large shell indices i ensure that large-index shells attract most nodes.

In order to express this model in exponential family form, define the set of natural parameters $\theta_i = \log(p_i/p_m)$. Note that, by definition, $\theta_m = 0$, so there are m linearly independent parameters; we will thus denote by $\theta = (\theta_0, \ldots, \theta_{m-1})$ the vector of natural parameters. The shell distribution ERGM can now be written in the following form:

$$P(G = g) = \exp\left\{\sum_{j=0}^{m-1} n_j(g)\theta_j - \psi(\theta)\right\}, \tag{3}$$

where $\psi(\theta)$ is the log-partition function (or the log normalizing constant), given by

$$\psi(\theta) = \log \sum_{g \in \mathcal{G}_{n,m}} \exp\left\{\sum_{j=0}^{m-1} n_j(g)\theta_j\right\}. \tag{4}$$

The m-truncated shell distribution $(n_0(g), \ldots, n_{m-1}(g))$ is a minimal sufficient statistic of the model. The natural parameter space is

$$\Theta = \{\theta \in \mathbb{R}^m : \psi(\theta) < \infty\} = \mathbb{R}^m. \tag{5}$$

Given this model specification, the overarching objective is to use it to perform statistical inference. However, as is usually the case for ERGMs, evaluating the log-partition function above is intractable for any reasonably sized N. This will affect the computation of the maximum likelihood estimator (MLE), requiring one to resort to MCMC methods, as well as testing model fit. In the remainder of this paper, we study three important aspects of these problems. First,

both MLE computation and model fitting depend on our ability to sample from the model with a given parameter value. To this end, we provide an MCMC algorithm for sampling from the model, summarize the results of several simulations, and provide an interpretation of the model parameters and the sampling distribution of realizable graph shell structures. Second, from the theory of exponential families, we know that the MLE is unique if it exists. But the question of existence is not often easy to address; we solve it here for the shell distribution model. Finally, testing model fit necessitates the ability to sample from the *fibers* of the model, that is, the subspaces of $\mathcal{G}_{n,m}$ with given fixed values of the shell distribution. We provide an algorithm for performing this task. We begin with theoretical considerations, then proceed to simulation results.

3.1. Sample space restriction and degeneracy of real-world networks

In ERGMs, sample space restriction leads to an improvement in the properties of the conditional model and estimation algorithms, as shown in Snijders and Van Duijn (2002), Snijders (2002). A usual approach is to condition on the degree sequence, maximum degree, or degree distribution, etc. In contrast, we are conditioning on the observed degeneracy of the graph. This is more robust than conditioning on the degrees, as we are allowing the degrees to be somewhat free but are still controlling sparsity in another way.

Degeneracy of real networks tends to be small relative to the number of nodes. A table illustrating this for the undirected graphs from the Pajek collection of datasets (Batagelj and Mrvar) is included below.

Network Dataset	#Nodes	#Edges	Degen.	Shell Distribution
Scotland	244	256	4	$(16, 26, 183, 7, 12)$
Geom	7343	11898	21	$(1185, 2218, 1714, 1023, 503, 248, 122, 126, 34, 27, 20, 52, 0, 1, 7, 14, 17, 0, 0, 0, 0, 22)$
NDyeast	2114	2277	5	$(244, 1199, 478, 169, 18, 6)$
NetScience	1589	2742	19	$(128, 320, 390, 281, 223, 89, 21, 60, 27, 30, 0, 0, 0, 0, 0, 0, 0, 0, 0, 20)$
USpowerGrid	4941	6594	5	$(0, 1588, 3122, 195, 24, 12)$
Erdős	6927	11850	10	$(0, 4780, 954, 466, 258, 179, 113, 73, 49, 17, 38)$

Observe that the degeneracy of the graph is allowed to grow as the number of nodes grows, but is expected to be significantly smaller than n in real-world networks.

4. Inference and implementation of the shell distribution ERGM

Many inference problems associated with ERGMs require generating random samples from the model at a fixed parameter value. In particular, problems such as computing an MLE using Monte Carlo methods (Snijders (2002)), sampling from the posterior distribution of the parameters (Caimo and Friel (2011)) and exploring the space of graphs that have high probability under the model each require random samples from the model. In this section, we present a commonly

used MCMC sampling algorithm to sample graphs from the shell distribution ERGM and use this algorithm to obtain maximum likelihood estimates and to understand the properties of random graphs that arise from the shell distribution ERGM.

Sampling from the shell distribution ERGM: As is the case with most ERGMs, sampling from the shell distribution ERGM is intractable and we need to resort to Markov chain Monte Carlo (MCMC) schemes. We use a Metropolis-Hastings algorithm with a tie-no-tie proposal (see Caimo and Friel (2011)) to generate graphs from the model. At each iteration, the algorithm proposes a graph g' from the current state g and decides to accept it with probability

$$\min\left(1, \frac{P(g') \cdot P(g' \to g)}{P(g) \cdot P(g \to g')}\right) = \min\left(1, \prod_i p_i^{n_i(g')-n_i(g)} \cdot \frac{P(g' \to g)}{P(g \to g')}\right), \quad (6)$$

where $\{g \to g'\}$ denotes the event that the Markov chain moves from g to g'. Note that when the proposed graph g' has degeneracy not equal to m, by definition of the model, $P(g') = 0$, hence the acceptance probability is 0.

A simple proposal distribution that is commonly used for proposing new graphs in the Metropolis framework is to randomly select a dyad and swap it. However, during experiments, we found that this leads to Markov chains with poor mixing properties. Instead, we use a "tie-no-tie" (TNT) proposal, also used in Caimo and Friel (2011). At each iteration, the TNT proposal randomly chooses between the set of edges and non-edges, and then swaps a randomly chosen dyad within the selected set. But this proposal is not symmetric: Let π be the probability of choosing the set of edges, $ne(g)$ be the number of non-edges in g and $e(g)$ be the number of edges in g. Then the Hastings ratio $\frac{P(g' \to g)}{P(g \to g')}$ is determined as follows:

$$\frac{P(g' \to g)}{P(g \to g')} = \begin{cases} \frac{\pi}{1-\pi} \frac{ne(g)}{e(g)+1}, & \text{if } g' \text{ is obtained from } g \text{ by adding an edge} \\ \frac{1-\pi}{\pi} \frac{e(g)}{ne(g)+1}, & \text{if } g' \text{ is obtained from } g \text{ by removing an edge.} \end{cases} \quad (7)$$

Remark 4. Computing the acceptance probability using Equation (6) requires one to compute the so-called vector of "change statistics" $\{n_i(g') - n_i(g)\}, i = 1, \ldots, n$ at each step, see Hunter and Handcock (2006). For many existing ERGMs, the change statistics can be computed locally, i.e without resorting to computing the sufficient statistics for proposed network g'. However, this is not the case for the shell distribution as it is a *global* sufficient statistic. In order to compute the change statistics, we need to recompute the shell distribution for the proposed network g' at each step of the Markov chain. This increases the computational complexity of the algorithm, even though one can compute the shell distribution in linear time.

4.1. Estimating the parameters of the shell distribution ERGM

A natural starting point to estimate parameter values θ and m using a real network is by either (a) using their observed counterparts, (b) by using a maximum likelihood estimate. We will discuss these two estimating methods for both θ and m. Estimation of m is tricky, as it represents the model dimension, and we observe only one graph. Also for any observed graph, allowing m to be different from the observed degeneracy leads to many undesirable properties of the resulting model. We explain this issue at length in Section 9.2. Thus for simulation studies based on real networks we fix m to be the observed degeneracy.

Estimation of θ is more involved. One can estimate θ naively by using the empirical shell distribution and setting $\hat{\theta}_j = n_j/n$, or one can use a more principled likelihood-based estimator (such as an MLE or a Bayes estimate). It turns out that using the observed shell distribution as an empirical estimate leads to a poor (or uninteresting) parameter estimate - in particular, networks sampled from the empirical estimate do not resemble the observed network. Namely, the model puts most of its mass on graphs with all nodes in the largest possible shell (see also Sections 4.2 and 4.3). On the other hand, computing an MLE of θ from the observed network is intractable due to the normalizing constant $\psi(\theta)$ given in Equation (4). Maximizing the likelihood requires the repeated use of Markov Chain Monte Carlo sampling, as described below, see also Hunter and Handcock (2006) and references therein. Bayesian estimates are also intractable due to two normalizing constants, see Caimo and Friel (2011) for more details.

We use Markov chain Monte Carlo MLE (Geyer and Thompson (1992); Snijders (2002)) to estimate θ. For $t = 0, 1, \ldots$, let θ^t be the parameter estimate at iteration t. We estimate the ratio of the intractable normalizing constant $\frac{\psi(\theta)}{\psi(\theta^t)}$ using samples from θ^t obtained by the Markov chain algorithm presented earlier. Specifically, let $g_1, \ldots, g_B$ be a random sample from the model θ^t, then

$$\frac{\psi(\theta)}{\psi(\theta^t)} \approxeq \frac{1}{B} \sum_{b=1}^{B} \exp\left\{(\theta - \theta^t) n_S(g_b)\right\}.$$

Then, θ^{t+1} is estimated by maximizing the estimated log-likelihood, given by

$$\hat{l}(\theta, \theta^t) = (\theta - \theta^t) n_S(g_{obs}) - \log \frac{\psi(\theta)}{\psi(\theta^t)}$$

and the process is repeated until convergence, see Hunter and Handcock (2006) for more details.

Estimation of the normalizing constant requires a good initial value θ_0 (Hunter and Handcock (2006)). We use a heuristic grid search to obtain a good starting point that is close to the MLE, where closeness to the MLE is evaluated by checking if the empirical version of the following moment equation holds:

$$E_{\hat{\theta}}[n_s(g)] = n_s(g_{obs}),$$

where g_{obs} is the observed graph and $\hat{\theta}$ is an MLE estimate.

The behavior of the MCMC-MLE estimator depends on the choice of a good starting point θ_0. For the current simulations, we use a heuristic starting point, but one could also consider the step length algorithm in Hummel et al. (2012) to find a good starting point close to the MLE.

What do graphs from the shell distribution ERGM look like? We use the MCMC algorithm described above to explore the structure of random graphs generated by the model for fixed and estimated parameter values. In particular, for a fixed choice of parameters θ and m of the shell distribution ERGM, we explore the space of graphs that have high probability mass under the model by sampling a large number of graphs $\{g_b\}_{b=1}^{B}$ using the MCMC algorithm. We use these samples to find out what features of any given network can be captured by modeling its core structure through the shell distribution ERGM. In the simulation studies below, we employ two types of parameter values to simulate graphs - known fixed parameters and parameters estimated from a real-world network. For the known parameters, we always use degeneracy $m = 3$. Parameter estimates based on real world networks are obtained using a combination of a heuristic grid search (to initialize the MCMC MLE algorithm) and MCMC MLE. To explore the sampled space of graphs, we summarize the distribution of the sampled graphs $\{g_b\}$ by using several summary statistics: boxplots of the degree distribution and shell distributions, and histograms of number of edges, two stars, and triangles, centrality, size of largest shell and size of the innermost shell. When the parameters are estimated using a real world network, we also compare the distribution of these summary statistics with the corresponding observed statistic. It may be tempting to use this comparison as a way to assess the goodness of fit of the model, however, one must exercise caution:

Remark 5. It is important to note that comparing the sampling distribution of summary statistics with the observed values is not a formal goodness-of-fit test of the model, but instead a heuristic approach to evaluate how well the model fits the data. It follows along the lines the goodness-of-fit testing proposed for more general ERGMs in Hunter et al. (2008). Ideally, one should be able to either derive the asymptotic distribution of any test statistic or, since in this case we usually observe a single network, perform an exact test. However, doing so requires several important steps, foremost, a good choice of a test statistic that can play the role of a generalized goodness-of-fit statistic. In case of, say, hierarchical log-linear models for contingency tables, one can use the chi-square statistic, and sample from the conditional distribution given the observed sufficient statistic to approximate the exact distribution of χ^2. In case of this ERGM, however, we do not have at our disposal such a statistic that can reliably 'measure' the distance of the observed network from the expected network. The main obstacle is that the dyads are not independent in this model, unlike the case of hierarchical models in which cells in the contingency table (arising from the incidence matrix) are independent. To this end, we follow the generally used strategies for ERGMs and report the sampling distributions

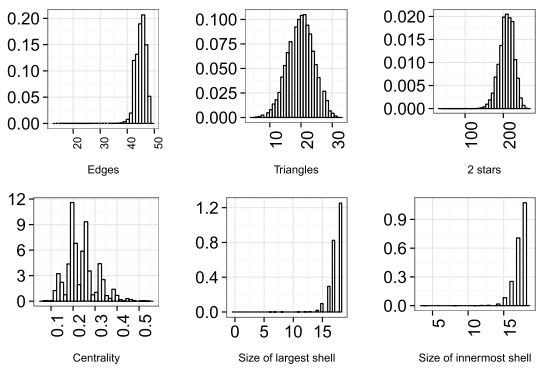

FIG 3. *Sampling distributions of summary statistics from the* Equal Attractiveness *model*

of various complementary network statistics, such as the number of edges and the number of triangles. For completeness, we explore the distribution of these statistics when conditioning on the sufficient statistics in Section 6.

4.2. Example 1: Various fixed Shell probabilities

In this section, we study the properties of the shell distribution ERGM by simulating graphs from various fixed parameters. We set $m = 3$, $n = 18$ and consider two models:

1. Equal attractiveness, i.e., $p_i = \frac{1}{4}$ for all i;
2. Decaying attractiveness, i.e, $p_i \propto e^{-i}$ for all i.

Equal attractiveness Model: This model posits that every shell has equal attractiveness, i.e. $p_i = \frac{1}{4}$ for all i and since $\theta_i = \log \frac{p_i}{p_m}$, it follows that $\theta = (0, 0, 0, 0)$. Hence by definition, this model places a uniform mass over the set of all 3-degenerate graphs. The sampling distribution of various summary statistics of graphs sampled from this model are shown in Figure 3. Note that even though the model posits that every shell has equal attractiveness a priori, the sampled graphs are such that most nodes tend to lie in the innermost shell which is shell 3 in this case. This can be seen by the histogram of the size of the innermost shell in Figure 3. There are at least three reasons for this behavior, the first one related to the very definition of the shell index. Namely, the existence of higher-index shells in a graph requires a certain minimum number of nodes in it, and hence, a priori, higher shells have higher levels of natural "attractiveness", to which we refer as intrinsic graph-theoretic attractiveness. In this sense, the innermost shell is always the most attractive. Secondly, the model puts a uniform distribution on the space of all graphs, not on the space of all shell distributions. For example consider the 4-truncated shell distributions $(0, 0, 0, 18)$ and $(18, 0, 0, 0)$: there are many graphs realizing the former, yet exactly one graph realizing the latter, namely the empty graph. Thus, the

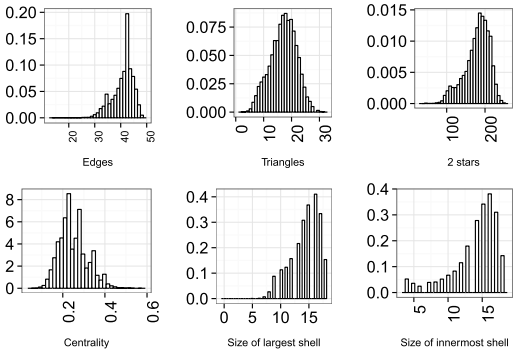

FIG 4. *Sampling distributions of summary statistics from the* Decaying Attractiveness *model*

sampling distribution of the shell distributions is non-uniform. Finally, there is also an issue with the slow mixing of the Markov chain. Shell distributions with a large number of nodes in the higher-indexed shells are "stable" in the sense that adding or removing a single edge tends to leave the shell distribution unchanged. On the other hand, when most nodes are in lower index shells, adding or removing a few edges lead to large changes in the shell distribution.

It is worth noting that the second and the third issue above are, in fact, related to each other and also to an issue that arises naturally in ERGMs in general. Namely, ERGMs model random graphs, not sufficient statistics, thus a uniform distribution over the set of graphs is not a uniform distribution over the set of sufficient statistics one may care about. This is made evident by the current example: a uniform distribution over 3-degenerate graphs induces a non-uniform distribution on the graph statistics such as number of triangles, number of edges, and 2-stars.

Decaying Attractiveness Model: The decaying attractiveness model posits that the attractiveness of each shell decays exponentially with its index, i.e. $p_i = ce^{-i}$, where c is some constant. This model aims to overcome the problems imposed by the intrinsic graph-theoretic attractiveness of the higher-index shells. Figure 4 shows the sampling distributions of summary statistics of the samples from this model. The histogram of the size of the innermost shell has two modes, one at 16 and a second one at 4, suggesting a bimodal distribution. The histograms of number of two stars and the number of triangles are bimodal as well.

4.3. Example 2: Sampson monastery data

The Sampson dataset is a widely studied network of size 18 that records interactions among a group of monks in a New England Monastery Sampson (1968) and their evolution over time. The first three time periods of the original Sampson data are commonly used (e.g., in the `ergm` package) and often aggregated. The network at any of these three time periods makes for an uninteresting example

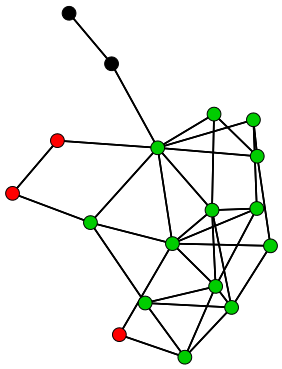

FIG 5. *A subset of the Sampson Monastery Dataset: Nodes are colored according to their shell index: black is* 1*, red is* 2*, and green is shell index* 3*.*

from the point of view of shells: namely all nodes are in the same shell and of degeneracy 3, but we have already considered such networks in Section 4.2. The aggregate network over the three time periods also has just about all nodes (all but 4) in the highest shell and is of degeneracy 5. In order to obtain a more varied shell distribution as a case study to examine the model behavior, we consider instead an arbitrary subgraph of the aggregate network; specifically, we use the upper triangular part of the adjacency matrix and symmetrize it. This undirected network is shown in Figure 5, color-coded by shells; it has $n = 18$ nodes, $e = 35$ edges and density of 0.23. The observed degeneracy is 3 and the observed 4-truncated shell distribution is $(0, 2, 3, 13)$; there are 3 nonempty shells, and the innermost shell (shell 3) contains the highest number of nodes (13).

To use this Sampson-derived network to study the properties of the shell distribution ERGM, we set $m = 3$ and use MCMC MLE to estimate the value of θ. Using a heuristic grid search, we found $\theta_0 = (2, 1, 1, 0)$ to be a good initial estimate. The estimated MLE is $\hat{\theta}_{MLE} = (-7.95, 2.79, 0.91, 0)$ which corresponds to $\hat{p}_{MLE} = (0.00, 0.82, 0.13, 0.05)$. Recall that $\theta_i = \log \frac{p_i}{p_m}$ and hence θ_i can be interpreted as the log-odds of attractiveness of shell i relative to shell m. For this dataset, attractiveness of shell 1 relative to shell 3 is almost 3 times that of shell 2, thus indicating that the network has a rich periphery in the sense of Rombach et al. (2014). This can also be seen by noting that $\hat{p}_1 = 0.82$; recall that the p_i can also be interpreted as the propensity of the i-th shell to have nodes in it beyond its intrinsic graph-theoretic attractiveness (as explained in Section 4.2).

Next, using $m = 3$ and the MLE estimate $\theta = (-7.95, 2.79, 0.91, 0)$, we simulated networks from the model using the MCMC algorithm presented earlier in this Section to study what properties of the network are captured by the model. One can think of these sampled graphs as samples from the posterior predictive distribution. Convergence of a 40,000-step Markov chain was verified using the usual diagnostics, such as trace plots and autocorrelation plots to ensure sufficient mixing. Figures 6, 7(a), 7(b) summarize the results of the simulations.

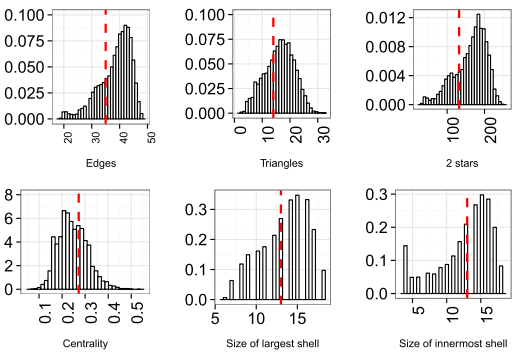

FIG 6. *Sampling distribution of summary statistics from the model estimated from the dataset in Figure 5. The red dashed lines indicate the observed values of the statistics.*

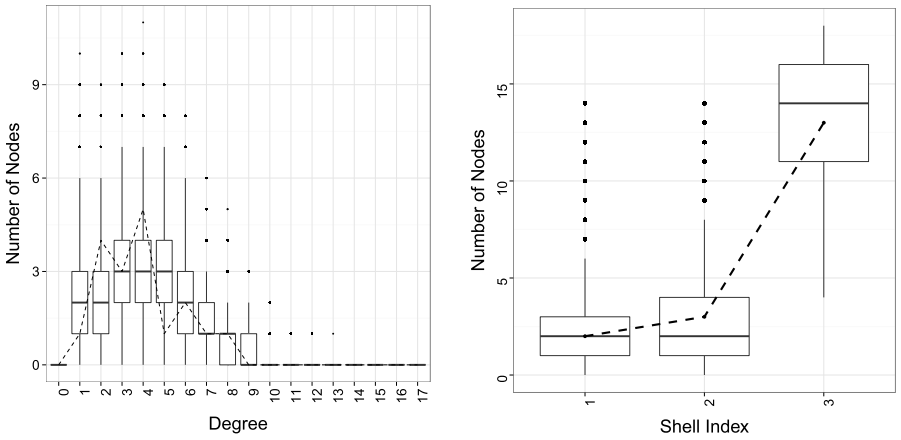

(a) Degree Distribution (b) Shell Distribution

FIG 7. *Box plots of degree distributions and shell distributions for the shell distribution model estimated from Sampson data. The dashed lines represent the observed distributions.*

Specifically, Figure 6 shows the sampling distribution of various summary statistics in the form of a histogram and compares them with the observed values. Several interesting results emerge. The sampling distribution of the summary statistics are all unimodal and very close to the observed statistic shown by the red line. Notice that the histogram of triangles is centered around the observed value, thus the shell distribution model captures triadic effects quite well, at least in this small example. We would like to draw a comparison with degree-based models which do not capture triadic effects, by definition. It is widely believed that the centrality of a network is related to its core distribution, and the histogram of centrality provides additional support of this hypothesis. The distribution of the size of the largest shell is also captured by the model. How-

TABLE 1
The top 10 visited shell distributions

Shell Distribution	Density (in %)
0.1.1.16	5.95
0.0.1.17	5.79
0.1.2.15	5.22
0.0.2.16	4.54
0.2.1.15	4.22
0.0.0.18	3.88
0.1.3.14	3.64
0.2.2.14	3.63
0.1.0.17	3.54
0.0.3.15	2.89

ever, the sampling distribution of number of edges suggests that the observed number of edges is much smaller than what we expect under the model. This may be due to the fact that the model has a bias towards graphs with higher-index shells (innermost cores), and these shells tend to be densely connected. A similar situation is true for the number of two-stars. The sampling distribution of the size of the innermost shell indicates that it can have anywhere from 5 to 18 nodes, with two modes at 15 and 16; compare this with the observed number of 13 nodes in shell 3. We also consider various shell distributions visited by the Markov chain. The top 10 most frequently visited shell distributions are given in Table 1.

Figures 7(a) and 7(b) show the box plots of degree and shell distributions, respectively, of the sampled graphs, and include the observed degree and shell distributions as dotted lines. Note that the sampling distribution of degree distributions is quite different from that of shell distributions, showing that the shell distribution model captures features that go beyond the degrees, and justifying our initial motivation for constructing the model. In addition, the sampling distribution of the shell distribution is concentrated around the observed shell distribution. This is to be expected: as we used the observed shell distribution to estimate the model, it serves as a check that the MLE of θ using MCMC MLE is indeed a good estimate. Recall that another definition of the MLE is the following: If $\hat{\theta}$ is an MLE, then, $E_{\hat{\theta}}[n_s(g)] = n_s(g_{obs})$. Figure 7(b) serves as a visual confirmation of this equation. In fact, the observed shell distribution is $n_s(g_{obs}) = (0, 2, 3, 13)$ and the estimate of the expected shell distribution (based on the MCMC samples from $\hat{\theta}$) turns out to be $\hat{E}_{\hat{\theta}}[n_s(g)] = (0.00, 2.29, 3.06, 12.66)$. Finally, even though the general trend in the observed degree distribution is captured by the model, as suggested by Figure 7(a), there is a substantial deviation between the observed degree distribution and the one suggested by the model. This reinforces the observation that the degree distribution and shell distribution capture different aspects of the Sampson network, and the shell distribution ERGM captures properties of the network beyond the degrees. In fact, it is well-known that degree-based models have independent dyads, whereas the shell distribution ERGM does not. This is further evidenced by Figure 6.

5. A sampling algorithm for generating graphs with a given shell distribution

In the last two decades, there have been several contributions in the graph theory and computer science literature on computing cores decompositions. Given the wide-ranging application of cores, a natural problem that arises is to find an algorithm that randomly generates graphs with a given core structure. Such an algorithm is presented in Baur et al. (2007) for graphs with additional restrictions on the number of edges between pairs of shells.

This section provides a simple algorithm (Algorithm 3) for sampling the space of graphs with a given shell distribution (sometimes called the *fiber* of that distribution), such that any graph has positive probability of being constructed (Theorem 9). This is an independent sampler, not a Markov chain. Simulations indicate good performance in terms of discovering new graphs at a fast pace. While the true sampling distribution is not known, our experiments show that reasonably long runs will give good estimates.

Algorithm 1: Compute Shell Sequence

input : a graph g
output: its shell sequence $s(g) = (s_1, \ldots, s_n)$

1 Initialize $s^* = 0$.
2 Repeatedly remove vertices of degree at most s^* in g, incrementing s^* by 1 if no eligible vertices remain in g; quit when g is empty. The shell index of each vertex is the value of s^* when it was deleted.

For convenience, we restate the basic algorithm for producing the shell sequence of a graph as Algorithm 1. There is no need to implement it, since the linear-time algorithm from Batagelj and Zaveršnik (2003) is already implemented as the `graph.coreness` function from the Csardi and Nepusz (2006) `igraph` package in `R`.

Note that the order in which the vertices of g are deleted in Algorithm 1 is neither unique, nor arbitrary: vertices are deleted in increasing order of their shell indices, but not all vertices with the same shell index are interchangeable. For example, consider the graph in Figure 2(a), for which every vertex has shell index equal to 1: the first vertex deleted will be, by necessity, one of the vertices of degree 1, but the second vertex deleted can vary depending on the choice of the first vertex.

Our sampling algorithm will generate graphs with vertices in an order that is compatible with Algorithm 1, so we will need to know more about such orderings. To that end, we give a simple condition for a graph g on vertices $\{v_1, \ldots, v_n\}$ that determines whether Algorithm 1 could potentially process its vertices in that order, yielding a pre-specified sorted shell sequence $s_1 \leq \ldots \leq s_n$.

Condition 6. For all $i \in [n]$:

(i) v_i has at least s_i neighbors v_j with $s_j \geq s_i$, and
(ii) v_i has at most s_i neighbors v_j with $j > i$.

Lemma 7. *Consider any graph $g \in G_n$ on vertices labeled $v_1, \ldots, v_n$ and sorted sequence of n non-negative integers $s_1 \leq \ldots \leq s_n$. Algorithm 1 can process the vertices of g in the given order, yielding shell indices $s(v_i) = s_i$ for all $i \in [n]$, if and only if g satisfies Condition 6.*

Proof. Consider Algorithm 1 on a graph g satisfying Condition 6, at the moment when s^* increments from $s-1$ to s. The subgraph induced by $\{v_i : s_i \geq s\}$ has minimum degree at least s by Condition 6(i), so none of those vertices can have been deleted yet. On the other hand, if v_i is the vertex remaining in g with smallest index i, then v_i must have at least s neighbors v_j with $j > i$, so by Condition 6(ii), $s_i \geq s$. Thus, the vertices remaining in g at that moment are precisely those v_i with $s_i \geq s$. Applying the argument for any s and for $s+1$ shows that the vertices v_i with $s_i = s$ are precisely those which Algorithm 1 deletes when $s^* = s$, as required.

For the other direction, suppose that Algorithm 1 processes the vertices of g in order, yielding $s(v_i) = s_i$ for all $i \in [n]$. Then Condition 6(ii) is true since $s^* = s_i$ when v_i is deleted. Suppose that Condition 6(i) is not true for some v_i. Just before s^* increments from $s_i - 1$ to s_i, all vertices v_j with $s_j < s_i$ have been deleted, so v_i has fewer than s_i neighbors remaining. Then v_i could be deleted, which would make its shell index $s_i - 1$ according to the algorithm, a contradiction. □

Given a sorted shell sequence $s_1, \ldots, s_n$ of some simple graph, we initially aim to construct a graph g in n steps, by adding edges from v_i to v_j with $j > i$ during Step i so that Condition 6 is satisfied. At Step i, we will need to know how many neighbors v_i already has with shell index at least s_i—call this number t_i. Then Condition 6 can be restated as follows: v_i has between $s_i - t_i$ and s_i new neighbors added during Step i, where $t_i = |\{v_j : v_j v_i \in g,\ j < i,\ s_j \geq s_i\}|$. These considerations are summarized in Algorithm 2.

Algorithm 2: Graph sampler: initial version

input : a sequence of non-negative integers $s_1 \leq \ldots \leq s_n$
output: a graph g on vertices $v_1, \ldots, v_n$ with shell sequence $s(g) = (s_1, \ldots, s_n)$

```
for i ← 1 to n do
    Make v_i adjacent to a set S of vertices v_j with j > i such that s_i − t_i ≤ |S| ≤ s_i
    Update t_j values as needed.
end
```

However, Algorithm 2 could get stuck if it is unable to choose S as required. This problem will not happen as long as the number of vertices v_j with $i < j \leq n$ is at least $s_i - t_i$. For Steps $i \leq n - s_n$, the number of such vertices $n - i$ satisfies $n - i \geq s_n \geq s_i \geq s_i - t_i$, so the problem can only occur for $i > n - s_n$. To avoid this, we will modify those steps of the algorithm.

Consider $i \geq n - s_n$. Since the number of vertices v_j with $j > i$ is $n - i \leq s_n$ and $s_i = s_n$, the condition $s_i - t_i \leq |S| \leq s_i$ reduces to just $|S| \geq s_n - t_i$. The number of vertices in $\{v_j : j \geq n - s_n\}$ is $s_n + 1$, including v_i, so v_i has s_n

potential neighbors in that set. Thus, for such i, Condition 6 is equivalent to Condition 8, which is as follows:

Condition 8. For all $i \in [n]$ with $i \geq n - s_n$, v_i has at most t_i non-neighbors in the set $\{v_j : n - s_n \leq j \leq n\}$.

As we process vertices v_i with $i \geq n - s_n$, let t'_i represent the maximum number of non-neighbors allowed among unprocessed vertices. Initialize $t'_i = t_i$ for all $n - s_n \leq i \leq n$. To satisfy Condition 8, each t'_j decreases by 1 whenever it is not made adjacent to the currently active vertex v_i. When a t'_j reaches zero, we make it adjacent to all remaining vertices and then remove v_j from further consideration; note that this does not change t'_i for any $i \neq j$. Since no t'_i will ever go below zero, we will be able to process all v_i with $i \geq n - s_n$ so that Condition 8 is satisfied.

Finally, recall that $t_i = |\{v_j : v_j v_i \in g,\ j < i,\ s_j \geq s_i\}|$. Since the given sequence $s_1, \ldots, s_n$ is sorted in increasing order, $s_j > s_i$ is impossible when $j < i$. Thus, an equivalent definition of t_i is:

$$t_i = |\{v_j : v_j v_i \in g,\ j < i,\ s_j = s_i\}|. \tag{8}$$

Algorithm 3 constructs graphs within the restrictions permitted by Condition 6 (for $i < n - s_n$) and Condition 8 (for $i \geq n - s_n$), choosing randomly among all possibilities whenever there is more than one option. As we have shown, the algorithm will never get stuck. Thus, we have the following result:

Theorem 9. *For any graph g with shell sequence $s(g)$, Algorithm 3 produces g, up to isomorphism, with positive probability.*

A comment on the running time of Algorithm 3: Since a random set R can be chosen from a given set S in $O(|S|)$ time, this algorithm runs in $O(|V|^2)$ time.

We conclude this section by summarizing simulation results. Algorithm 3 randomly constructs both labeled graphs (which requires permuting the node labels of the output of the algorithm) and unlabeled graphs with a given shell distribution. It produces graphs in every isomorphism class of the shell distribution, and our simulations give preliminary evidence that it also does so quite fast.

As an example, consider shell distribution $(0, 2, 1, 4, 0, 0, 0)$ on 7 vertices. For labeled graphs, 10,000 runs of the algorithm produced more than 7,400 distinct graphs, which implies a very high discovery rate of the fiber. For unlabeled graphs, discovering the 12 isomorphism classes requires only 100 calls to the algorithm.

6. Behavior of complementary statistics on the fiber of the shell ERGM

In this section, we explore—both theoretically and experimentally—the behavior of various subgraphs on the fiber of graphs with a given shell distribution. In the network literature, subgraphs—such as edges and triangles—are used to perform heuristic goodness-of-fit tests. Hence, understanding how these subgraphs

Algorithm 3: Graph Sampler: construct a random graph with a given shell sequence

input : a sorted integer sequence $s_1 \leq \ldots \leq s_n$
output: a graph g with shell sequence $s(g) = (s_1, \ldots, s_n)$

Initialize $v_1, \ldots, v_n$ to be the vertices of g.
Initialize $t_1 = \ldots = t_n = 0$
for $i \leftarrow 1$ **to** $n - s_n - 1$ **do**
  Choose a random subset R of $\{v_j : i < j \leq n\}$ with $\max\{0, s_i - t_i\} \leq |R| \leq s_i$
  for $v_j \in R$ **do**
    Add the edge $v_i v_j$ to g
    if $s_j = s_i$ **then** $t_j \leftarrow t_j + 1$
  end
end
Initialize $S = \{v_j : n - s_n \leq j \leq n\}$
for $v_j \in S$ **do**
  if $t_j = 0$ **then**
    $S \leftarrow S \setminus \{v_j\}$
    Add edges from v_j to all $v_k \in S$ in g
  end
end
while $S \neq \emptyset$ **do**
  Pick any $v_i \in S$
  $S \leftarrow S \setminus \{v_i\}$
  Choose a random subset R of S with $|R| \geq |S| - t_i$
  for $v_j \in R$ **do**
    Add the edge $v_i v_j$ to g
  end
  for $v_j \in S \setminus R$ **do**
    $t_j \leftarrow t_j - 1$
    if $t_j = 0$ **then**
      $S \leftarrow S \setminus \{v_j\}$
      Add edges from v_j to all $v_k \in S$ in g
    end
  end
end

can vary across the set of graphs with a fixed shell distribution is important. We present the results in terms of a *sorted shell sequence*, but note that a sorted shell sequence is equivalent to a shell distribution, as one can be obtained from the other uniquely. The following are lower and upper bounds on the number of edges and triangles in a graph with a prescribed shell sequence and degeneracy m.

Proposition 10. *If g is a graph with sorted shell sequence $s_1 \leq \ldots \leq s_n$, then the maximum number of edges in g is*

$$\binom{m}{2} + \sum_{i=1}^{n-m} s_i.$$

Proof. By Lemma 7, each vertex v_i has at most s_i neighbors v_j with $j > i$, and the total number of v_j with $j > i$ is $n - i$. We will construct a graph so that the

first bound is realized for v_i with $i \leq n - m$ and the second bound is realized for $i \geq n - m$; thus, it has the maximum possible number of edges.

Begin with a complete graph G_0 on the m highest indexed vertices, $v_{n-m+1}, \ldots, v_n$. Then for each $1 \leq i \leq n - m$, add exactly s_i edges from v_i to $V(G_0)$. This yields a graph with the desired number of edges. □

Proposition 11. *If g is a graph with sorted shell sequence $s_1 \leq \ldots \leq s_n$ and corresponding shell distribution $n_S(g) = (n_0, \ldots, n_{n-1})$, then the minimum number of edges in g is*

$$\sum_{j=1}^{m} f(n_j, j),$$

where

$$f(n_j, j) = \begin{cases} \lceil \frac{jn_j}{2} \rceil & \text{if } j < n_j \\ jn_j - \binom{n_j}{2} & \text{if } j \geq n_j. \end{cases}$$

Proof. For any $0 \leq i \leq m$, the vertices with shell index i must have at least i neighbors in $\{v_j : s_j \geq i\}$. We will construct a graph in stages as j ranges from m down to 0, adding vertices with shell index j during stage j, using the minimum possible number of edges to satisfy the previous condition.

First, given any $d < n$, we show how to construct a graph $G(n, d)$ with n vertices, minimum degree d, and the fewest possible number of edges. Let the vertex set be Z_n and arrange the vertices evenly around a circle. If d is even, make each vertex adjacent to the $d/2$ closest vertices to it on either side. If d is odd and n is even, make each vertex adjacent to the $(d-1)/2$ closest vertices to it on either side and also to the vertex directly across from it. If d is odd and n is odd, there is no d-regular graph on n vertices, but we can construct an n-vertex graph with one vertex of degree $d+1$ and all other vertices of degree d, as follows: Begin by making each vertex adjacent to the $(d-1)/2$ closest vertices to it on each side. Then, for $0 \leq i \leq \frac{d-1}{2}$, make vertex i adjacent to vertex $i + \frac{d+1}{2}$. Note that for $i = \frac{d-1}{2}$, we get an edge from vertex $\frac{d-1}{2}$ to vertex $d \equiv 0 \bmod n$. The degree of vertex 0 increases by two and every other vertex degree increases by one, as required. Note that the number of edges in $G(n, d)$ is $\lceil nd/2 \rceil$.

Now, start with $G(n_m, m)$, which we can do since $n_m \geq m + 1$. Next we consider j starting from $j = m - 1$ down to $j = 0$, adding n_j vertices with shell index j at each step as follows: If $n_j > j$, then we add a disjoint copy of $G(n_j, j)$. If $n_j \leq j$, we add a disjoint complete graph on n_j vertices and, from each of its vertices, add edges to exactly $j - n_j + 1$ other vertices (which were added at earlier steps).

Let $f(n_j, j)$ be the number of edges added in Step j. Then $f(n_j, j) = \lceil jn_j/2 \rceil$ when $j < n_j$ and

$$f(n_j, j) = \binom{n_j}{2} + n_j(j - n_j + 1) = jn_j - \binom{n_j}{2}$$

when $j \geq n_j$.

The minimum number of edges is thus $\sum_{j=1}^{k} f(n_j, j)$. □

The following proposition provides a sharp upper bound on the number of triangles.

Proposition 12. *The maximum number of triangles for a graph with sorted shell sequence $s_1 \leq \ldots \leq s_n = m$ is*

$$\binom{m}{3} + \sum_{i=1}^{n-m} \binom{s_i}{2}.$$

Proof. The construction in the proof of Proposition 10 produces a graph with the correct number of triangles and the argument is similar. □

Obtaining an explicit lower bound for the number of triangles is difficult. Instead, we construct graphs with the given shell sequence with relatively few triangles, thus providing an upper bound for the minimum number of triangles for graphs with the specified shell sequence. The first construction begins with a complete graph on m vertices but then minimizes additional edges added in subsequent steps.

Lemma 13. *Let $s_1 \leq \ldots \leq s_n$ be a sorted shell sequence. Then, there exists a graph g with this shell sequence and exactly A triangles, where*

$$A = \binom{s_n}{3} + \sum_{i=\max(1,n-2s_n+1)}^{n-s_n} \binom{s_i}{2}.$$

Proof. Start with a complete graph on vertices $S_0 := \{v_i : n - s_n + 1 \leq i \leq n\}$. Let $S_1 := \{v_i : \max(1, n - 2s_n + 1) \leq i \leq n - s_n\}$ and for each $v_i \in S_1$, add exactly s_i edges from v_i to S_0. Finally, for $1 \leq i \leq n - 2s_n$, add to the graph a vertex v_i and exactly s_i edges from v_i to S_1. □

The idea in the next construction is to grow a (nearly balanced) bipartite graph with partite sets S, S' rapidly. However, it may be impossible to make a bipartite graph, so we maintain another set S_0 for the vertices that cannot be placed into S or S'. Every triangle will have at least one vertex in S_0.

Fix any sorted shell sequence $s_1 \leq \ldots \leq s_n = m$. If $n_m \geq 2m$, let $S_0 = \emptyset$, let S, S' be sets of sizes $\lfloor n_m/2 \rfloor, \lceil n_m/2 \rceil$, and let G be the complete bipartite graph with partite sets S, S'.

Otherwise, $m+1 \leq n_m < 2m$. Let $a_0 = 2s_n - n_m$ and let $a_m = a'_m = n_m - s_n$, then let S_0, S, S' be vertex sets of sizes a_0, a_m, a'_m respectively. Initialize G to be the union of a complete graph on S_0 and the complete tripartite graph with partite sets S_0, S, S'. Note that G has n_m vertices and minimum degree s_n.

Starting with $j = m - 1$ and decreasing j after each step, add n_j vertices to $S \cup S'$, split so that that $|S| - |S'|$ is 0 or ± 1. Make each new vertex in S adjacent to j vertices in S' if $|S'| \geq j$. Otherwise, make each new vertex in S adjacent to every vertex in S' and also adjacent to $j - |S'|$ vertices in S_0; this adds $\binom{j-|S'|}{2}$ triangles per new vertex in S. Similarly add j edges from each new

vertex of S' to vertices in S if possible or to vertices in $S \cup S_0$ otherwise, which adds $\binom{j-|S|}{2}$ triangles per new vertex of S'. Let B be the number of triangles in the graph obtained.

Although we cannot give a simple formula for B, we can compute B directly, without actually constructing the graph: If $n_m \geq 2n$, then $B = 0$. Otherwise, $m + 1 \leq n_m < 2m$. In that case, we use a_j, a'_j to represent the sizes of S, S' after step j, where j is initialized to be m and then decreases after each step. The number of new vertices in S, S' in each step is represented by x, x'. Then the computation can be performed as written in Algorithm 4.

Algorithm 4: Compute B, the number of triangles in the above graph construction

if $n_m \geq 2n$ **then** $B \leftarrow 0$
else
  Initialize $j \leftarrow m$, $a_0 \leftarrow 2s_n - n_m$, $a_m = a'_m \leftarrow n_m - s_n$, and $B \leftarrow \binom{a_0}{3} + \binom{a_0}{2}(a_m + a'_m) + a_0 a_m a'_m$
  while $j > 1$ **do**
    Let $j \leftarrow j - 1$
    if n_j *is even* **then** $x \leftarrow n_j/2$ and $x' \leftarrow n_j/2$
    else if $a_{j+1} > a'_{j+1}$ **then** $x \leftarrow \lfloor n_j/2 \rfloor$ and $x' \leftarrow \lceil n_j/2 \rceil$
    else $x \leftarrow \lceil n_j/2 \rceil$ and $x' \leftarrow \lfloor n_j/2 \rfloor$
    $a_j \leftarrow a_{j+1} + x$ and $a'_j \leftarrow a'_{j+1} + x'$
    $B \leftarrow B + x\binom{j-a'_j}{2} + x'\binom{j-a_j}{2}$ `/* where` $\binom{k}{2} = 0$ `whenever` $k < 2$ `*/`
  end

Moreover, if ever $\min(j - a'_j, j - a_j) < 2$, then B will remain fixed thereafter, since j is decreasing and a_j and a'_j are increasing evenly. Thus, the algorithm can be terminated early if $\min(j - a'_j, j - a_j) < 2$.

Proposition 14. *Let $s_1 \leq \ldots \leq s_n$ be a sorted shell sequence. Then, the minimum number of triangles in a graph with this shell sequence is at most* $\min\{A, B\}$.

Proof. This follows immediately from Lemma 13 and the previous construction. □

In order to further understand the behavior of these subgraph counts on the fibers of the model, we simulated graphs using Algorithm 3 with the shell distribution corresponding to the Sampson network studied above. Here, we summarize the results of those simulations.

Recall that the 4-truncated shell distribution of the Sampson network is $(0, 2, 3, 13)$. The network has 35 edges and 14 triangles. Simulating 50,000 graphs with this shell distribution using Algorithm 3 produced graphs with as many as 41 and as few as 27 edges. Propositions 10 and 11 show that the maximum and minimum number of edges for graphs with this shell distribution are 44 and 24, respectively. The maximum number of triangles among the simulated graphs was 30, and the minimum was 0. The upper bound for the number of triangles

in a graph with this shell distribution, as given by Proposition 12, is 34. The value A in Lemma 13 is 0, which coincides exactly with the minimum number of triangles observed in the simulations.

It is worth noting that, among the 50,000 simulated graphs with shell distribution corresponding to that of the Sampson network, no two were isomorphic. In other words, 50,000 calls to Algorithm 3 produced 50,000 distinct graphs. This again suggests that Algorithm 3 discovers the fiber of graphs with a fixed shell structure at a high rate.

7. Existence of MLE and the model polytope

It is well-known from the theory of exponential families (e.g., classical text Brown (1986)) that the MLE of the natural parameters of the model exists if and only if the average sufficient statistic of the sample lies in the interior of the convex polyhedron from the following definition. For discrete exponential families, and ERGMs in particular, Rinaldo et al. (2009) offer details on the relevance of this polyhedron to the problem of maximum likelihood estimation and study its properties from both theoretical and algorithmic point of view.

Definition 15. The *model polytope* (or *marginal polytope*) for the shell distribution ERGM defined in Equations (3) and (4) with the sufficient statistic vector $(n_0(g), \ldots, n_{m-1}(g))$ is the convex hull of all possible vectors of minimal sufficient statistics:

$$\mathcal{P}_{n,m} = \text{conv}\{(n_0(g), \ldots, n_{m-1}(g)) | g \in \mathcal{G}_{n,m}\} \subset \mathbb{R}^m.$$

Of course, each value of m gives rise to a different polytope, but each turns out to be a subpolytope (in fact, a face, as explained below) of the one with unrestricted degeneracy $m \leq n-1$. Thus we define it as a special case and study its geometry first. For simplicity of notation, denote the minimal sufficient statistic vector of the unrestricted model (i.e., the truncated shell distribution) by $n_S^*(g) = (n_0(g), \ldots, n_{n-2}(g))$.

Definition 16. The model polytope for the shell distribution ERGM with unrestricted degeneracy is

$$\mathcal{P}_n := \text{conv}\{n_S^*(g) | g \in \mathcal{G}_n\} \subset \mathbb{R}^{n-1}.$$

Denote by $\bar{n}_S^*$ the *average sufficient statistic* of the sample $g_1, \ldots, g_N$; its j^{th} entry is $\frac{1}{N}\sum_{j=1}^{N} n_j^*(g_i)$.

Proposition 17. *For a sample of size $N = 1$, $\bar{n}_S^*$ never lies in the interior of $\mathcal{P}_n$; that is, the MLE never exists.*

Proof. Determining whether $\bar{n}_S^*$ lies in the relative interior of $\mathcal{P}_n$ or on its boundary requires an explicit description of the polytope. We will show that $\mathcal{P}_n$ is a

dilate of a simplex. To this end, let us consider the polytope of non-truncated shell distributions:

$$P_n = \text{conv}\{(n_0, \ldots, n_{n-1}) : \\ (n_0, \ldots, n_{n-1}) = n_S(g) \text{ for some } g \in \mathcal{G}_n\}.$$

We claim that $(n_0, \ldots, n_{n-1}) = n_S(g)$ for some $g \in \mathcal{G}_n$ if and only if $n_m \geq m+1$ and $\sum n_j = n$, where $m = \text{dgen}(g)$.

That $n_m \geq m+1$ is a necessary condition is clear by definition. To show that it is sufficient, it suffices to construct a graph g with this sequence. But this is straightforward: starting with K_m, add $n_m - m$ vertices and connect each of them with every vertex of K_m. This gives the m-shell. Then, to construct the j-shell for all other j, simply add as many vertices as are necessary in the shell, and connect each of them with j edges to some subset of the original K_m.

Listing all integer points of this polytope, it is not difficult to see that it is simply an n-dilate of the simplex, $P_n = \text{conv}\{ne_i\} = n\Delta_{n-1} \subset \mathbb{R}^n$, where e_i is the i-th standard unit vector in $\mathbb{R}^n$. Finally, to obtain the polytope $\mathcal{P}_n$ with the truncated sequences, simply omit the last coordinate from P_n. The only effect this has on the polytope is that it interprets the simplex Δ_{n-1} as living in $\mathbb{R}^{n-1}$, instead of the way it is written above, as a polytope in $\mathbb{R}^n$ but embedded in the hyperplane $\sum_j n_j = n$.

Finally, note that all realizable integer points (i.e., those corresponding to a shell distribution) lie on the boundary of this polytope, and not its relative interior, since any realizable integer point must have a 0 in some component, as is evident from the necessary and sufficient conditions for shell distribution realizability given above. Thus, the MLE never exists for a single observation g. □

Remark 18. In case of larger samples, the MLE may or may not exist. The decision requires checking if the average sufficient statistic is on the boundary of $\mathcal{P}_n$.

We have shown that the polytope for unrestricted degeneracy model, $\mathcal{P}_n$, is just a dilate of the simplex, and all of the realizable sufficient statistics lie on its boundary. But the simple structure of $\mathcal{P}_n$ also implies that $\overline{\mathcal{P}_{n,m}} \subset \mathcal{P}_n$ for each $m \leq n-1$, where $\overline{\mathcal{P}_{n,m}}$ denotes the embedding of $\mathcal{P}_{n,m}$ into $\mathbb{R}^{n-1}$. Indeed, any point $p \in \mathcal{P}_{n,m} \subset \mathbb{R}^m$ corresponds to a point $\overline{p} \in \mathbb{R}^{n-1}$ which is clearly a realizable shell distribution vector. Thus $\overline{p}$ is a point in the polytope $\mathcal{P}_n$ that lies on the face cut out by the equations that set all coordinates other than the m-th one to zero.

Remark 19. Setting the degeneracy parameter m to be equal to the degeneracy of the observed graph and using the corresponding ERGM defined in Equations (3) and (4) with sample space $\mathcal{G}_{n,m}$ behaves better than using unrestricted degeneracy $m \leq n-1$ in general. In particular, many of the points that lie on the boundary of $\mathcal{P}_n$ lie on the relative interior of a face of some $\mathcal{P}_{n,m}$, thus the MLE has a positive probability of existing. The asymptotics of this construction are of interest to the behavior of the MLE problem, but are beyond the scope of the present paper.

8. Discussion

Cores have been widely used to study and summarize networks. In this paper we study the core decomposition of a network with an eye towards statistical inference. We embed the core structure of a network as captured by its shell distribution in the exponential random graph framework. We examine the theoretical properties of the model and study the problem of inference in the model which boils down to three tasks–existence of the MLE, sampling from the model and sampling from the fiber. The existence of MLE question is answered by characterizing the model polytope. To enable maximum likelihood estimation, we introduce a new type of support restriction that avoids bad behavior of the model common to many other classes of ERGMs. We develop an MCMC algorithm to sample from the model and apply this algorithm to estimate the MLE and perform heuristic goodness-of-fit tests. We also study the fibers of the model, i.e., spaces of graphs given a fixed shell distribution, and develop a sampling algorithm that can generate any graph with a predefined core structure with positive probability. Further, we describe the fiber in detail by computing bounds on subgraph counts induced by fixing the core structure of a network.

Our experiments and theoretical results indicate that the shell distribution model captures information beyond the degree distribution and, in particular, the triadic effects quite well. The model support is obtained by conditioning on the degeneracy of a graph. Conditioning is common in ERGMs, as it improves model properties and stability of estimation algorithms. The choice of degeneracy and thus the specific shell ERGM depends on the data and is meant to provide a way to improve not only the model's stability, but also its interpretability.

There are several interesting extensions of this work worth pursuing. Inference in the shell distribution ERGM gives rise to several important problems that deserve attention. One of the first considerations is computational: even though the shell distribution of a network can be computed in linear time, when embedded in an MCMC algorithm to compute change statistics, this process is very slow. In contrast, the change statistics of most ERGMs can be computed locally, without the need of recomputing the new sufficient statistic of the entire graph. A natural question to ask is if one can compute the change statistics of the shell distribution more efficiently. In particular, the following is of critical interest: *is there a way to use the local change in the network, such as adding or deleting edges, to re-compute the shell distribution?*

A related question is on the proposal distribution used in the MCMC algorithm. Since we restrict the support of the model to graphs with degeneracy equal to m, it would be useful to find proposal distributions that generate networks that are always in this set. We considered one type of summary statistic of the core distribution, namely the shell distribution and studied the associated ERGM thoroughly. Other interesting ways to summarize the core structure can be used to develop ERGMs. As mentioned, ERGMs based on the core distribution go beyond the dyadic assumption that is inherent in the degree-based

analysis. An interesting summary statistic to consider is the degree of a node in its core.

In a different direction, for many datasets, including the Sampson dataset, the network in question is directed. Notions of core decomposition can be defined for such generalizations of graphs as well: for example, the (k,l)-core of Giatsidis et al. (2013) for directed graphs. It is not difficult to extend our model and algorithms to this notion of core decomposition, and it would be interesting to see how that model would perform.

Finally, the support restriction applied to the core ERGM may be useful in other contexts, but a natural question to ask is how does one select the degeneracy parameter m.

9. Appendix A

This appendix deals with the case when graph degeneracy m is not restricted to one value for all graphs under the model. In other words, the unrestricted model gives positive probability to networks of degeneracy *less than or equal to* any fixed value of $m \leq n-1$. For simplicity, we will refer to this as the *unrestricted* model, motivated by the sample space restrictions placed in defining the core distribution ERGM in Section 3. We will see that the choice of any particular such $m \leq n-1$ does not affect the behavior of the model; instead, problems arise when allowing degeneracy to vary within the graphs in the model. Section 9.1 introduces the unrestricted model, which is ill-behaved (cf. Remark 3). Section 9.2 explains this behavior.

9.1. The model with unrestricted degeneracy

For completeness, let us re-derive the model, from first principles, for the unrestricted case $m \leq n-1$, for which the sample space is the set of all graphs with n nodes, $\mathcal{G}_n$.

Again, to take advantage of the theory of exponential families, we rewrite Equation (1) in exponential family form by re-parameterizing $P(G=g)$ in terms of normalized probabilities $\tilde{p}_j = \frac{p_j}{p_{n-1}}$. (Our notation very closely follows Sadeghi and Rinaldo (2014).)

Observe that $p_{n-1} = \frac{1}{1+\sum_{j=1}^{n-2}\tilde{p}_j}$, and thus $P(G=g)$ can be written as

$$\begin{aligned} P(G=g) &= \varphi(p)\prod_{j=0}^{n-1}(\tilde{p}_j p_{n-1})^{n_j(g)} = \varphi(p)p_{n-1}^{\sum_{j=0}^{n-1} n_j(G)}\prod_{j=0}^{n-1}\tilde{p}_j^{n_j(g)} \\ &= \varphi(p)p_{n-1}^{n}\prod_{j=0}^{n-1}\tilde{p}_j^{n_j(g)}, \end{aligned}$$

or, more compactly, using that $\tilde{p}_{n-1}=1$ and renaming the constant $\varphi(p)$ to

$\phi(\tilde{p})$ to reflect the re-parametrization:

$$P(G=g) = \frac{\phi(\tilde{p})}{\left(1+\sum_{j=1}^{n-2}\tilde{p}_j\right)^n}\prod_{j=0}^{n-2}\tilde{p}_j^{n_j(g)}. \tag{9}$$

Next, let $\theta_j = \log\tilde{p}_j$ and define the normalizing constant in terms of θ as $\psi(\theta) = n\log(1+\sum_{j=0}^{n-2}\exp(\theta_j)) - \log(\phi(\tilde{p}))$. With this, we can write $P(G=g)$ in exponential family form:

$$P(G=g) = \exp\left\{\sum_{j=0}^{n-2} n_j(g)\theta_j - \psi(\theta)\right\}. \tag{10}$$

For this version of the model, the minimal sufficient statistic is given by the truncated shell distribution $n_S^*(g) = (n_0(g),\ldots,n_{n-2}(g))$. As before, it is not difficult to see that the natural parameter space Θ for the model is $\Theta = \mathbb{R}^{n-1}$.

To obtain the log-partition function $\psi(\theta)$ in closed form, for fixed n, consider the set of graphs on n nodes as an ordered list, $\mathcal{G}_n = \{g_1 = K_n, \ldots, g_i, \ldots, g_M = \bar{K}_n\}$, where the graphs are listed in non-increasing order in terms of the number of edges, and where $M = 2^{\binom{n}{2}}$. Note that in the empty graph g_M, every vertex has shell index 0, while in the complete graph $g_1 = K_n$, the shell indices are $s(v) = n-1$ for all $v \in V(K_n)$. Therefore,

$$P(G=g_M) = \frac{\phi(\tilde{p})}{\left(1+\sum_{j=0}^{n-2}\tilde{p}_j\right)^n}\cdot\tilde{p}_0^n, \tag{11}$$

and

$$P(G=g_1) = \frac{\phi(\tilde{p})}{\left(1+\sum_{j=0}^{n-2}\tilde{p}_j\right)^n}. \tag{12}$$

For any other arbitrary graph $g_i \in \mathcal{G}_n \setminus \{\bar{K}_n, K_n\}$,

$$P(G=g_i) = \frac{\phi(\tilde{p})}{\left(1+\sum_{j=1}^{n-2}\tilde{p}_j\right)^n}\prod_{j=0}^{n-2}\tilde{p}_j^{n_j(g_i)}. \tag{13}$$

Using $\sum_{i=1}^{M} P(G=g_i) = 1$ and Equations (11) and (13), the normalizing constant $\phi(\tilde{p})$ can be rewritten as:

$$\phi(\tilde{p}) = \frac{\left(1+\sum_{j=0}^{n-2}\tilde{p}_j\right)^n}{1+\ldots+\prod_{j=0}^{n-2}\tilde{p}_j^{n_j(g_i)}+\ldots+\tilde{p}_0^n}. \tag{14}$$

Finally, $\theta_j = \log\tilde{p}_j$ and the second equality in (11) provide $\psi(\theta) = \log(1+\ldots+\prod_{j=0}^{n-2}\tilde{p}_j^{n_j(g_i)}+\ldots+\tilde{p}_0^n) = \log(1+\ldots+e^{\sum_{j=0}^{n-2} n_j(g_i)\theta_j}+\ldots+e^{n\theta_0})$.

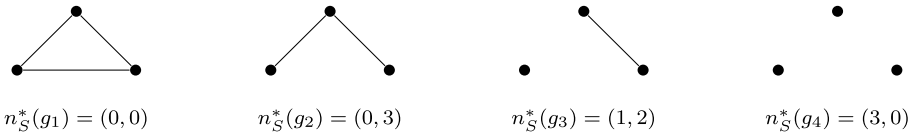

FIG 8. *Truncated shell distributions of all non-isomorphic simple graphs on* 3 *vertices.*

Example 20. Determining $\psi(\theta)$ for the case $n = 3$ depends on counting simple graphs on three nodes up to isomorphism. Namely, there are 4 non-isomorphic simple graphs on 3 vertices (see Figure 8): $\mathcal{G}_n$ consists of 1 copy of g_1, 3 isomorphic copies of g_2, 3 isomorphic copies of g_3 and 1 copy of g_4. For $g_1 = K_3$, each vertex has shell index 2, so $n_S^*(g_1) = (0,0)$. For g_2, each vertex has shell index 1 and therefore $n_S^*(g_2) = (0,3)$. Two vertices of g_3 have shell index 1 while the remaining vertex has shell index 0, so $n_S^*(g_3) = (1,2)$, and $n_S^*(g_4) = (3,0)$ as every vertex of $g_4 = \bar{K}_3$ has shell index 0. Therefore, the log-partition function for $n = 3$ is $\psi(\theta) = \log(1 + 3\tilde{p}_1^3 + 3\tilde{p}_0\tilde{p}_1^2 + \tilde{p}_0^3) = \log(1 + 3e^{3\theta_1} + 3e^{2\theta_1+\theta_0} + e^{3\theta_0})$.

9.2. Bad behavior of the unrestricted model

In this subsection we illustrate how the model misbehaves if the degeneracy m is not controlled. The model with unrestricted degeneracy allows, for any fixed m, the support of the model to contain graphs with degeneracy less than or equal to m, i.e. the sample space of the model is defined as follows:

$$\mathcal{G}_{n,\leq m} = \{g \in \mathcal{G}_n : \mathrm{dgen}(g) \leq m\}.$$

Note that a special case is when $\mathcal{G}_{n,\leq n-1} = \mathcal{G}_n$, that is, a graph with *any* degeneracy is allowed with positive probability under the model.

If we allow the model to put positive mass on graphs with degeneracy less than or equal to m, then for any generic point in the parameter space Θ, the following behavior occurs: The likelihood function has many modes, and the local modes of the model corresponding to graphs where all nodes lie in the shells that are most popular (with respect to the m^{th} shell). Example 21 illustrates this point, followed by Lemma 22 that makes this intuitive explanation of the model behavior precise.

Example 21. Let $m = 4$ and consider the unrestricted shell ERGM supported on the sample space $\mathcal{G}_{n,\leq 4}$, i.e., the model puts a positive mass on all graphs with degeneracy less than or equal to 4. Let $\theta = (\theta_0, \ldots, \theta_4)$ be a parameter vector of this model. Recall that $\theta_i = \log \frac{p_i}{p_m}$ and hence $\theta_4 = 0$. Without significant loss of generality, let us assume that $\theta_3 > \theta_0, \theta_1, \theta_2$. Hence amongst shells 0, 1, 2 and 3, the 3^{rd} shell has the highest attractiveness, relative to the 4^{th} shell. Consider the set of graphs whose degeneracy is less than $m = 4$, i.e. $\mathcal{G}_{n,\leq 3}$. Let g be any graph in $\mathcal{G}_{n,\leq 3}$, then $n_s(g) = (n_0(g), n_1(g), n_2(g), n_3(g), 0)$. Let g^* be any graph in $\mathcal{G}_{n,\leq 3}$, where all nodes lie in the shell 3, which is the most attractive shell, i.e., $n_s(g^*) = (0, 0, 0, n, 0)$.

Then $P(g^*) > P(g)$. Indeed, the following inequalities are straightforward:

$$\begin{aligned}\log \frac{P(g^*)}{P(g)} &= \sum_{i=0}^{m-1} \theta_i (n_i(g^*) - n_i(g)) \\ &= -\sum_{i=0}^{m-2} \theta_i n_i(g) + \theta_{m-1} \left(n - n_{m-1}(g)\right) \\ &= -\sum_{i=0}^{m-2} \theta_i n_i(g) + \theta_{m-1} \left(\sum_{i=0}^{m-2} n_i(g)\right) \\ &= \sum_{i=0}^{m-2} n_i(g)(\theta_{m-1} - \theta_i) > 0.\end{aligned}$$

This should be interpreted as follows: Among the set of all graphs with degeneracy less than or equal to 3, the most likely graph will be such that all nodes are in the shell index corresponding to the largest θ. Thus, in some sense, the local mode is a "degenerate" mode (no pun intended!).

In the above example, we could have chosen any θ_k, $k \neq m$, to be the most attractive shell, and the shell distribution of g^* should be modified accordingly, i.e. $n_k(g^*) = n$ and $n_i(g^*) = 0$ for all $i \neq k$. Moreover, we could have considered the mode over any restricted sample space, not just $\mathcal{G}_{n,\leq 3}$. Lemma 22 illustrates this point by generalizing the example in several directions, in particular, by allowing there to be more than one 'popular' shell. Let m be the degeneracy of the model, let $\theta = (\theta_0, \ldots, \theta_{m-1})$ be the parameter vector of the shell ERGM. Define $[m] = \{0, 1, \ldots, m-1\}$.

Lemma 22. *Consider the shell ERGM on the sample space $\mathcal{G}_{n,\leq m}$ with parameter vector $(\theta_0, \ldots, \theta_m)$, where $\theta_m = 0$ by definition. Let g be any graph in $\mathcal{G}_{n,\leq d}$ with degeneracy $d < m$, i.e., $n_i(g) = 0$ for all $i > d$. Let $\mathcal{L}_d = \{l \in [d] : \theta_l = \max_{i\in[d]} \theta_i\}$. Let $\mathcal{L}_d^c = [d] \backslash \mathcal{L}_d$. Let g^* be any network with degeneracy d such that nodes exist only in the most popular shells, i.e. $n_i(g^*) = 0$ for all $i \notin \mathcal{L}_d$.*

Then, $P(g^*) > P(g)$.

Proof. Let $\theta^* = \max_{i\in[d]} \theta_i$, and consider the following, as in Example 21:

$$\begin{aligned}\log \frac{P(g^*)}{P(g)} &= \sum_{i\in[d]} \theta_i (n_i(g^*) - n_i(g)) \\ &= \sum_{i\in\mathcal{L}_d^c} \theta_i (0 - n_i(g)) + \sum_{i\in\mathcal{L}_d} \theta_i \left(n_i(g^*) - n_i(g)\right) \\ &= -\sum_{i\in\mathcal{L}_d^c} \theta_i n_i(g) + \theta^* \sum_{i\in\mathcal{L}_d} \left(n_i(g^*) - n_i(g)\right) \\ &= -\sum_{i\in\mathcal{L}_d^c} \theta_i n_i(g) + \theta^* \left(n - \sum_{i\in\mathcal{L}_d} n_i(g)\right)\end{aligned}$$

$$= -\sum_{i\in\mathcal{L}_d^c} \theta_i n_i(g) + \theta^* \left(\sum_{i\in\mathcal{L}_d^c} n_i(g)\right)$$
$$= \sum_{i\in\mathcal{L}_d^c} n_i(g)(\theta^* - \theta_i) > 0.$$

The fourth equality holds since $n_i(g^*) = 0$ for all $i \in \mathcal{L}_d^c$. The fifth equality holds because $\sum_{i\in[d]} n_i(g) = n$. □

As an additional example of behavior explained in Lemma 22, let $m = 5$, $d = 3$ and let $\theta = (a, \alpha, b, \alpha, c, 0)$ where $\alpha > a, b, c$. By Lemma 22, among all graphs with degeneracy at most 3, graphs with shell distribution $(0, k, 0, n-k, 0, 0)$ are the modes, where $n - k \geq 4$. Thus, among d-degenerate graphs, only graphs where all nodes lie in the most popular shells are modes. These graphs are vastly different from each other in terms of their topological properties (e.g. density, number of triangles), yet they occur as modes of the same parameter vector.

The reason why such a behavior occurs is that allowing graphs with degeneracy less than m introduces a linear constraint on the shell distributions of these graphs. Thus to eliminate such a behavior, we define the model so that any graph with degeneracy less than m has 0 probability. Two consequences of this fact are that when fitting the shell ERGM to an observed graph, (1) m cannot be larger than the observed degeneracy, and (2) graphs with degeneracy less than the observed degeneracy have 0 probability.

To see why (1) holds, let g be an observed graph with shell distribution $n_s(g)$ and degeneracy $\hat{m}$. Consider fitting the shell ERGM to g by allowing $m > \hat{m}$. If the sample space is $\mathcal{G}_{n,m}$, the observed graph has 0 probability under the model! On the other hand, if we let the sample space be $\mathcal{G}_{n,\leq m}$ and we have $\hat{m} < m$, the observed network lies in the set $\mathcal{G}_{n,\leq\hat{m}} \subsetneq \mathcal{G}_{n,\leq m}$. Lemma 22 can be applied to show that the model has an undesirable property. Let $\text{supp}(n_S) = \{i \in [m] : n_i(g) \neq 0\}$ be the support of n_S. Let Θ_g be a subset of the parameter space such that indices of largest value of θ correspond to $\text{supp}(n_S)$, i.e.,

$$\Theta_g = \{\theta \in \Theta : \forall s \in \text{supp}(n_S), \theta_s = \max_{i\in[m]} \theta_i\}$$

By Lemma 22, any parameter in Θ_g will have the observed graph g as one of its modes. Moreover, these models will have several other modes that have shell distributions quite different from the observed graph.

The above discussion shows that if we allow $m > \hat{m}$, there exist a large subset of the parameter space where the model misbehaves. A natural question to ask is the converse - does there exists a parameter vector for which the observed graph is the only mode? An easy algebraic calculation in Example 23 shows even a weaker requirement of having the model assign higher mass to graphs with shell distributions vastly different from the observed shell distribution is not possible.

Example 23. Let the observed shell distribution be $n_S(g) = (0, k, 0, n-k)$, with $n-k \geq 4$ and $k > 0$. Hence the observed degeneracy is $\hat{m} = 3$. Consider the shell ERGM with $m = 3$ and sample space $\mathcal{G}_{n,\leq 4}$. Consider two graphs g_1 and g_2 with shell distributions $(0, 0, n, 0)$ and $(0, n, 0, 0)$. We will show that there does not exist any point in the parameter space such that $P(g) > P(g_1)$ and $P(g) > P(g_2)$ simultaneously. To this end, let $\theta = (\theta_0, \theta_1, \theta_2, 0)$ be any point in the parameter space. Note that $\log \frac{P(g)}{P(g_1)} = (\theta_1 - \theta_3)k$ and $\log \frac{P(g)}{P(g_2)} = (\theta_3 - \theta_1)(n-k)$. For both these terms to be positive at the same time, we need $\theta_1 > \theta_3$ and $\theta_3 > \theta_1$ which is impossible. Moreover if $\theta_1 = \theta_3$, then the model places equal probability on the observed graph g and g_1 and g_2, which is undesirable.

Acknowledgements

The authors would like to thank Stephen Fienberg and Alessandro Rinaldo for several useful discussions on this topic and the anonymous reviewers for their careful reading of our paper and their suggestions for clarifications. Petrović, Stasi and Wilburne were supported by AFOSR/DARPA grant FA9550-14-1-0141. Karwa gratefully acknowledges support by a grant from the Singapore National Research Foundation under the Interactive and Digital Media Programme Office to the Living Analytics Research Centre.

References

José Ignacio Alvarez-Hamelin, Luca Dall'Asta, Alain Barrat, and Alessandro Vespignani. k-core decomposition: a tool for the visualization of large scale networks. In *Advances in Neural Information Processing Systems 18*, page 41. MIT Press, 2006. MR2395238

Joonhyun Bae and Sangwook Kim. Identifying and ranking influential spreaders in complex networks by neighborhood coreness. *Physica A: Statistical Mechanics and its Applications*, 395:549–559, 2014. MR3133686

Michael J. Bannister, William E. Devanny, and David Eppstein. ERGMs are Hard. Preprint, available at arxiv: arXiv:1412.1787 [cs.DS].

Vladimir Batagelj and Andrej Mrvar. Pajek datasets. URL `http://vlado.fmf.uni-lj.si/pub/networks/data/`.

Vladimir Batagelj and Matjaž Zaveršnik. An O(m) algorithm for cores decomposition of networks. *CoRR*, cs.DS/0310049, 2003.

Michael Baur, Marco Gaertler, Robert Görke, Marcus Krug, and Dorothea Wagner. Generating graphs with predefined k-core structure. *Proceedings of the European Conference of Complex Systems*, 2007.

Francesho Bonchi, Franceso Gullo, Andreas Kaltenbrunner, and Yana Volkovich. Core decomposition of uncertain graphs. *Proceedings of the 20th ACM SIGKDD International Conference on Knowledge Discovery and Data Mining*, 2014.

Lawrence Brown. *Fundamentals of Statistical Exponential Families*, volume 9 of *Monograph Series*. IMS Lecture Notes, 1986. MR0882001

Alberto Caimo and Nial Friel. Bayesian inference for exponential random graph models. *Social Networks*, 33(1):41–55, 2011. MR2873466

Shai Carmi, Shlomo Havlin, Scott Kirkpatrick, Yuval Shavitt, and Eran Shir. A model of internet topology using k-shell decomposition. *Proceedings of the National Academy of Sciences, USA*, 104:11150–11154, 2007.

Sourav Chatterjee and Persi Diaconis. Estimating and understanding exponential random graph models. *The Annals of Statistics*, 41(5):2428–2461, 2013. MR3127871

Sourav Chatterjee, Persi Diaconis, and Allan Sly. Random graphs with a given degree sequence. *Ann. Appl. Probab.*, 21(4):1400–1435, 2011. MR2857452

Gabor Csardi and Tamas Nepusz. The igraph software package for complex network research. *InterJournal*, Complex Systems:1695, 2006.

Marius Eidsaa and Eivind Almaas. s-core network decomposition: A generalization of k-core analysis to weights. *Physical Review*, 88(6):062819, 2013.

Charles J. Geyer and Elizabeth A. Thompson. Constrained monte carlo maximum likelihood for dependent data. *Journal of the Royal Statistical Society. Series B (Methodological)*, pages 657–699, 1992. MR1185217

Christos Giatsidis, Dimitrios M. Thilikos, and Michalis Varzigiannis. D-cores: measuring collaboration of directed graphs based on degeneracy. *Knowledge and Information Systems*, 35(2):311–343, 2013.

Anna Goldenberg, Alice X. Zheng, Stephen E. Fienberg, and Edoardo M. Airoldi. A survey of statistical network models. *Foundations and Trends in Machine Learning*, 2(2):129–233, 2009.

Steven M. Goodreau, James A. Kitts, and Martina Morris. Birds of a feather, or friend of a friend? using exponential random graph models to investigate adolescent social networks*. *Demography*, 46(1):103–125, 2009.

Paul W. Holland and Samuel Leinhardt. An exponential family of probability distributions for directed graphs. *Journal of the American Statistical Association*, 76(373):33–50, 1981. MR0608176

Ruth M. Hummel, David R. Hunter, and Mark S. Handcock. Improving simulation-based algorithms for fitting ergms. *Journal of Computational and Graphical Statistics*, 21(4):920–939, 2012. MR3005804

David R. Hunter and Mark S. Handcock. Inference in curved exponential family models for networks. *Journal of Computational and Graphical Statistics*, 15(3), 2006. MR2291264

David R. Hunter, Steven M. Goodreau, and Mark S. Handcock. Goodness of fit of social network models. *Journal of the American Statistical Association*, 103(481), 2008. MR2394635

Maksim Kitsak, Lazaros K. Gallos, Shlomo Havlin, Fredrik Liljeros, Lev Muchnik, Eugene H. Stanley, and Hernán A. Makse. Identification of influential spreaders in complex networks. *Nature Physics*, 6(11):888–893, 2010.

Michael M. Lee, Indrajit Roy, Alvin AuYoung, Vanish Talwar, K.R. Jayaram, and Yuanyuan Zhou. Views and transactional storage for large graphs. *Middleware*, pages 287–306, 2013.

Daniele Miorandi and Frencesco De Pellegrini. K-shell decomposition for dynamic complex networks. *Modeling and Optimization in Mobile Ad Hoc and*

Wireless Networks WiOpt 2010 Proceedings of the 8th International Proceedings on, pages 488–496, 2010.

Sofia C. Olhede and Patrick Wolfe. Degree-based network models. Preprint, arXiv:1211.6537, 2012.

Sen Pei, Lev Muchnik, Jose Andrade Jr., Zhiming Zheng, and Hernán Maske. Searching for superspreaders if information in real-world social media. *Nature Scientific Reports*, 4, 2012.

Alessandro Rinaldo, Stephen E. Fienberg, and Yi Zhou. On the geometry of discrete exponential families with application to exponential random graph models. *Electronic Journal of Statistics*, 3:446–484, 2009. MR2507456

Alessandro Rinaldo, Sonja Petrović, and Stephen E. Fienberg. Maximum lilkelihood estimation in the β-model. *The Annals of Statistics*, 41(3):1085–1110, 2013. MR3113804

Garry Robins, Pip Pattison, Yuval Kalish, and Dean Lusher. An introduction to exponential random graph (p*) models for social networks. *Social networks*, 29(2):173–191, 2007.

M. Puck Rombach, Mason A. Porter, James H. Fowler, and Peter J. Mucha. Core-periphery structure in networks. *SIAM Journal of Applied Math*, 74(1):167–190, 2014. MR3165913

Kayvan Sadeghi and Alessandro Rinaldo. Statistical models for degree distributions of networks. *NIPS Workshop*, 2014.

Samuel Franklin Sampson. *A novitiate in a period of change: An experimental and case study of social relationships*. PhD thesis, Cornell University, September, 1968.

Zachary M. Saul and Vladimir Filkov. Exploring biological network structure using exponential random graph models. *Bioinformatics*, 23(19):2604–2611, 2007.

Michael Schweinberger. Instability, sensitivity, and degeneracy of discrete exponential families. *Journal of the American Statistical Association*, 106(496):1361–1370, 2011. MR2896841

Stephen B. Seidman. Network structure and minimum degree. *Social Networks*, 5(3):269–287, 1983. MR0721295

Cosma Rohilla Shalizi, Alessandro Rinaldo, et al. Consistency under sampling of exponential random graph models. *The Annals of Statistics*, 41(2):508–535, 2013. MR3099112

Tom A.B. Snijders. Markov chain Monte Carlo estimation of exponential random graph models. *Journal of Social Structure*, 3(2):1–40, 2002.

Tom A.B. Snijders and Marijtje A.J. Van Duijn. Conditional maximum likelihood estimation under various specifications of exponential random graph models. *Contributions to social network analysis, information theory, and other topics in statistics*, pages 117–134, 2002. MR3074604

Tom A.B. Snijders, Philippa E. Pattison, Garry L. Robins, and Mark S. Handcock. New specifications for exponential random graph models. *Sociological methodology*, 36(1):99–153, 2006.

Stefan Wuchty and Eivind Almaas. Peeling the yeast protein network. *Proteomics*, 5(2):444–449, 2005.